



Lawrence Berkeley Laboratory

UNIVERSITY OF CALIFORNIA

Materials & Chemical Sciences Division

RECEIVED
LAWRENCE
BERKELEY LABORATORY

MAY 10 1988

LIBRARY AND
DOCUMENTS SECTION

Submitted to Journal of the Electrochemical Society

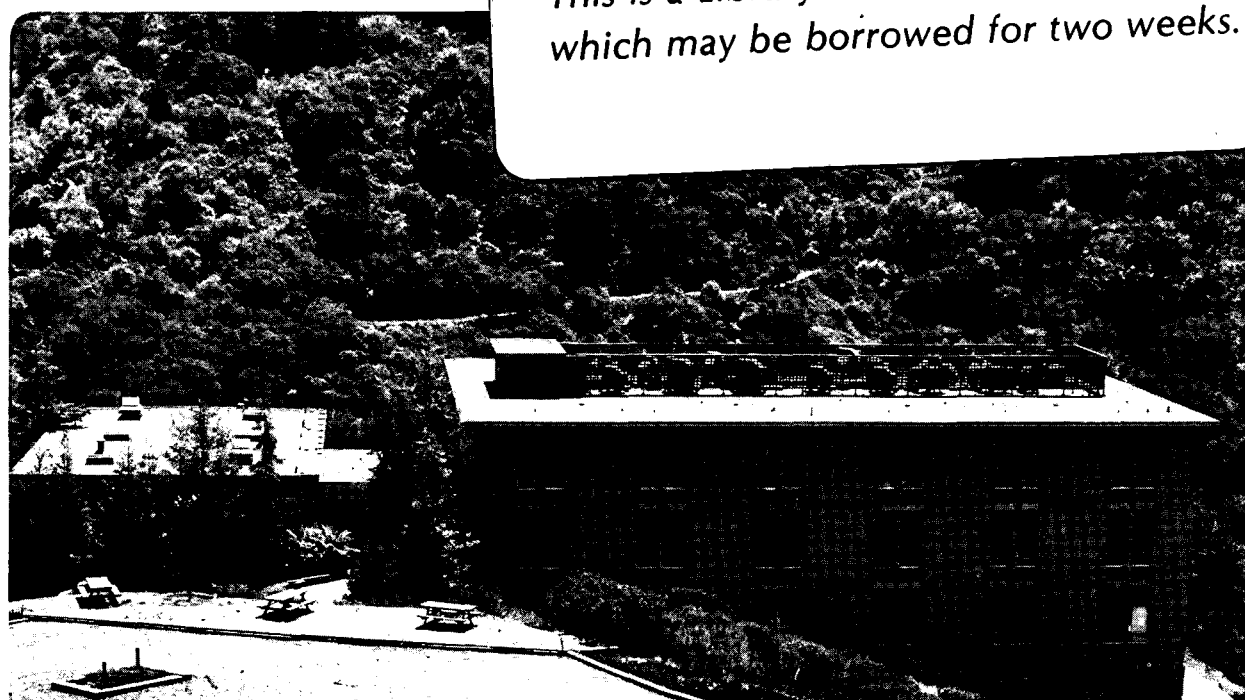
Current Distribution at Electrode Edges at High Current Densities

W.H. Smyrl and J. Newman

September 1987

TWO-WEEK LOAN COPY

*This is a Library Circulating Copy
which may be borrowed for two weeks.*



LBL-23905
c.2

DISCLAIMER

This document was prepared as an account of work sponsored by the United States Government. While this document is believed to contain correct information, neither the United States Government nor any agency thereof, nor the Regents of the University of California, nor any of their employees, makes any warranty, express or implied, or assumes any legal responsibility for the accuracy, completeness, or usefulness of any information, apparatus, product, or process disclosed, or represents that its use would not infringe privately owned rights. Reference herein to any specific commercial product, process, or service by its trade name, trademark, manufacturer, or otherwise, does not necessarily constitute or imply its endorsement, recommendation, or favoring by the United States Government or any agency thereof, or the Regents of the University of California. The views and opinions of authors expressed herein do not necessarily state or reflect those of the United States Government or any agency thereof or the Regents of the University of California.

Current Distribution at Electrode Edges
at High Current Densities

William H. Smyrl¹

Sandia National Laboratories
Albuquerque, New Mexico 87185
and

John Newman

Materials and Chemical Sciences Division, Lawrence Berkeley Laboratory,
and Department of Chemical Engineering, University of California,
Berkeley, California 94720

September 29, 1987

Abstract

At current densities large in magnitude and also large compared to the exchange current density, a conducting disk in an insulating plane has a very nonuniform current distribution across the surface. The current distribution near the center is governed predominantly by ohmic effects, but near the edge, electrode kinetics become important. This paper describes the treatment of the current and potential distributions on the electrode, especially near the edge of the electrode where the nonuniformity is most extreme. The electrode kinetics are taken to be in the Tafel region. The results are valid for any and all large values of current density and provide a definitive

¹Present address: Department of Chemical Engineering and Materials Science, University of Minnesota, Minneapolis, Minnesota 55455.

Key words: Laplace's equation, plating, potential distribution, Tafel kinetics, linear kinetics, high exchange currents.

description of the way in which the current and potential distributions approach the purely ohmically controlled (primary) distributions as the current is increased. The current density at the edge of the disk is found to increase with the square of the average current density.

These results for the edge region of a disk at high currents and those of an earlier paper for high exchange currents can be applied to electrodes of more general geometry.

Introduction

Current and potential distribution calculations have been used for many years in electroplating, electromachining, battery development, and corrosion. Such calculations allow one to predict the shape of metal deposition or removal during the progress of the process. The work represents an application of classical techniques of mathematical physics and as such has attracted the attention of the mathematician and physicist as well as the electrochemist and engineer. In recent years, the interest in such calculations has also been stimulated by the development of numerical techniques for use on high-speed digital computers, and a much wider variety of problems has been studied. The discussion here will present results of one of these computer-aided calculations.

Many of the early analytic calculations were made for a simplified limiting case, *i.e.*, for only ohmic conditions between the electrodes with no limitation from either diffusion or heterogeneous

electrode kinetics. A uniform current distribution on the electrodes was calculated for concentric spheres, concentric cylinders (neglecting end effects), a hemisphere on an insulating plane with the counterelectrode at infinity, and electrodes which completely filled the cross section of a cylindrical or rectangular tube. These important geometries have been used extensively in electrochemical research. Otherwise, the results showed extreme nonuniformity in the current distribution, with the current density approaching infinity at electrode edges and coplanar intersections with insulators. The more general case has been the nonuniform distribution.

The extreme nonuniformity shown for ohmic conditions will be moderated by electrode kinetics, which eliminates any infinite current densities and is the subject of the present paper. One can see the effect of electrode kinetics by referring to the relationship for Tafel kinetics, here for anodic current

$$\frac{i_n}{i_0} = \exp\left[\frac{\alpha_a F}{RT}(V - \Phi_0)\right] = \exp\left[\frac{\alpha_a F}{RT} \eta_s\right], \quad (1)$$

where i_n is the current density, i_0 the exchange current density, and α_a is the transfer coefficient. V is the electrode potential, Φ_0 is the potential in the solution adjacent to the surface, and η_s is the surface overpotential. If the current density were to approach infinity, the surface overpotential would approach infinity as well. This will not be realized experimentally, since the potential must remain bounded. Thus the current density at the edge of an electrode would remain finite. The moderating effect of electrode kinetics on the

edge region of a disk in an insulating plane is the specific system to be discussed here.

Newman¹ calculated the primary current distribution for a circular disk in a large, insulating plane and found it to be

$$\frac{i_n}{i_{avg}} = \frac{0.5}{\left(1 - r^2/r_0^2\right)^{1/2}} \quad (2)$$

It may be seen that as r approaches r_0 , the outer radius of the disk, the current density approaches infinity, although the total current to the disk remains finite. Newman² also calculated the current and potential distributions for a rotating disk in a plane under conditions where both kinetics and diffusion were specifically accounted for. It was shown² that the relative effects of kinetics and ohmic drop can be represented by the following dimensionless parameters:

$$J = \frac{(\alpha_a + \alpha_c)Fr_0}{RT\kappa} i_0 \quad (\text{for linear kinetics})$$

$$\delta = \frac{\alpha_a Fr_0}{RT\kappa} \left| i_{avg} \right| \quad (\text{for Tafel kinetics}) .$$

The current and potential distributions were shown to depend on either J or δ , depending upon kinetics, or both J and δ , and α_a/α_c as well, when neither the linear nor Tafel approximation could be used for the electrode kinetics. When J and δ were small, electrode kinetics were found to be dominant as compared to ohmic effects, and the current distribution on the electrode became uniform even though the primary distribution was nonuniform (equation 2). For large J or δ , the current distribution approached the primary distribution. The distri-

bution was calculated² for a number of values of J and δ , as well as for situations where diffusion was important. Nanis and Kesselman³ also made calculations for uniform and primary distributions for the rotating disk. Neither of these papers included a treatment of just how the current distribution approached the ohmically-determined, primary distribution for large J or δ . A subsequent finite-difference technique was described⁴ for calculating the current and potential distribution of a disk in a plane (where the surrounding plane could be either an insulator or an electrode), but again without describing the distributions for large J or δ .

Figure 1 reveals the difficulty in treating the edge region by finite-difference methods. The current distribution for a large value of δ ($\delta = 90$) has been calculated approximately by the finite-difference method and compared to the primary distribution, where the surrounding plane is an insulator. The rapid change of current density near the outer edge of the disk necessitates a large number of mesh points in this region, which is a small part of the entire region, and the problem would become more severe at larger δ . In the region near the center of the disk, the current distribution (for $\delta = 90$) approached the ohmic (primary) distribution. This suggested that approximations valid at the center of the disk were different from those valid at the edge; or expressed a different way, the effect of kinetic limitations was important only near the outer edge of the disk where the current was largest, and the current and potential distributions near the center were almost completely determined by ohmic

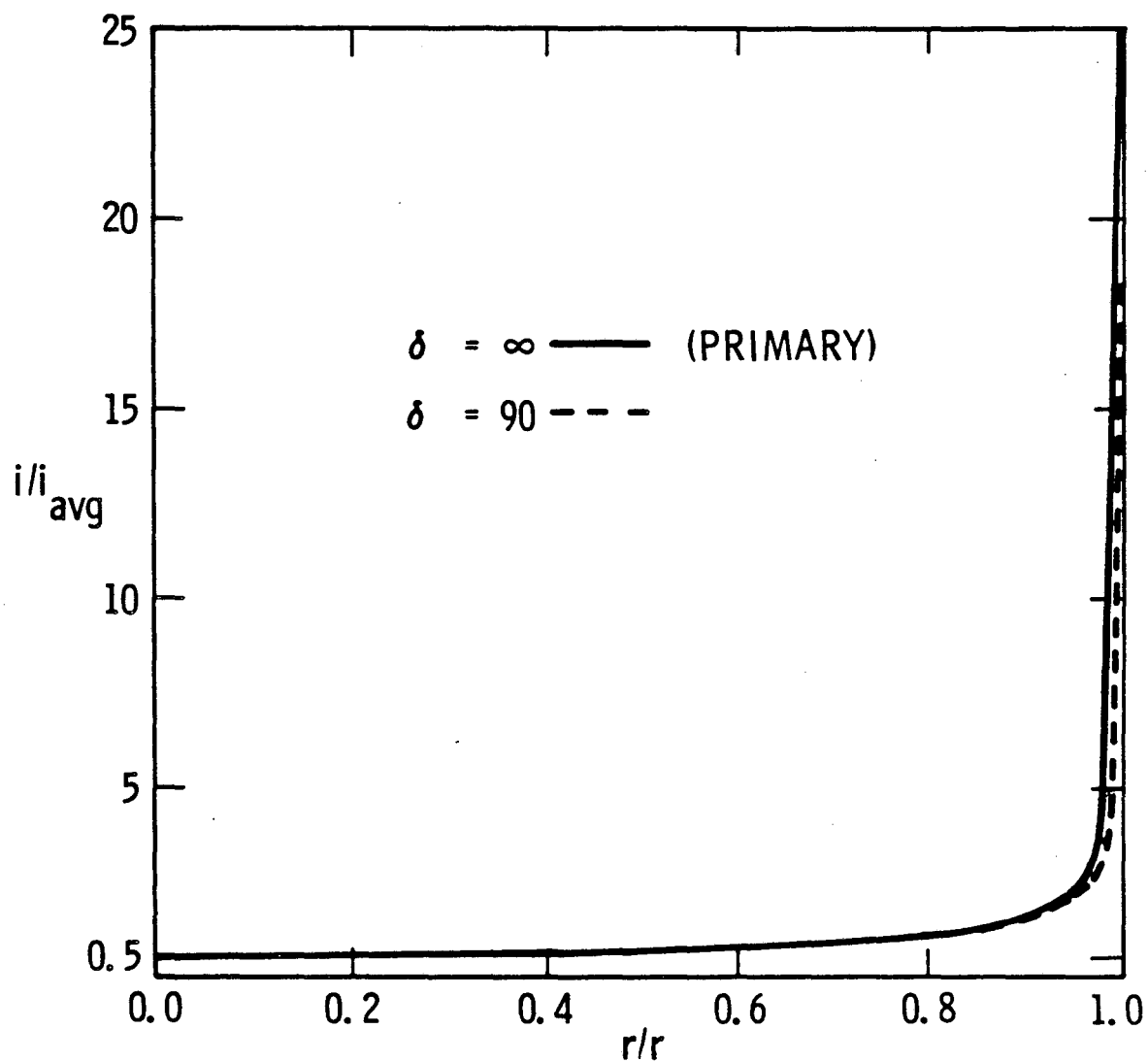


FIGURE 1. PRIMARY CURRENT DISTRIBUTION ON A DISK COMPARED TO THE DISTRIBUTION CALCULATED FOR A LARGE VALUE OF THE POLARIZATION PARAMETER FOR TAFEL KINETICS

effects.

In the analogous problem for linear kinetics at large J , Nişancıoğlu and Newman⁵ recognized the need for a singular-perturbation treatment. They found that the current (or potential) distribution became identical with the primary distribution near the center of the disk and that the current density at the edge depended on J as

$$\frac{i_{edge}}{i_{avg}} = 0.62 \sqrt{J} . \quad (3)$$

It can be seen that the current density at the edge approached infinity as J approached infinity.

The present paper will describe the results of the treatment of the current distribution for large values of δ . A singular-perturbation technique was used to set up the problem, which was solved by a numerical, finite-difference method. The problem is somewhat more complicated than that for large J ,⁵ as shown below, and the results of the two will be compared although they treat different kinetic boundary conditions. Comparison will also be made with early results of Wagner,⁶ who briefly discussed edge effects for situations close to the ohmic limit. We expect that the present treatment may be used along with that for large J for practical application in electrochemical machining.

Mathematical Treatment

Rotational elliptic coordinates have been used for the disk-plane geometry^{1,2,4,5} and will be adopted here. These coordinates, ξ, η , discussed extensively in reference 7, are related to cylindrical coordinates by

$$z = r_0 \eta \xi \quad (4)$$

$$r/r_0 = [(1 + \xi^2)(1 - \eta^2)]^{1/2} . \quad (5)$$

The disk-plane system is shown in the new coordinate system in figure 2. Also shown is the corner region where kinetics is important on the disk at high δ values. Laplace's equation in rotational elliptic coordinates is

$$(1-\eta^2) \frac{\partial^2 \Phi}{\partial \eta^2} + (1+\xi^2) \frac{\partial^2 \Phi}{\partial \xi^2} + 2\xi \frac{\partial \Phi}{\partial \xi} - 2\eta \frac{\partial \Phi}{\partial \eta} = 0 . \quad (6)$$

A solution to equation 6 was sought subject to the boundary conditions:

a. on the disk ($\xi = 0$), the current density is related to the potential derivative by

$$i_n = - \frac{\kappa}{r_0 \eta} \left. \frac{\partial \Phi}{\partial \xi} \right|_{\xi=0} . \quad (7)$$

For Tafel kinetics i_n is also related to the local electrode overpotential $V - \Phi_0$ by equation 1.

b. on the surrounding plane ($\eta = 0$), an insulator surface,

$$i_n = 0 = - \frac{\kappa}{r_0 \xi} \left. \frac{\partial \Phi}{\partial \eta} \right|_{\eta=0} . \quad (8)$$

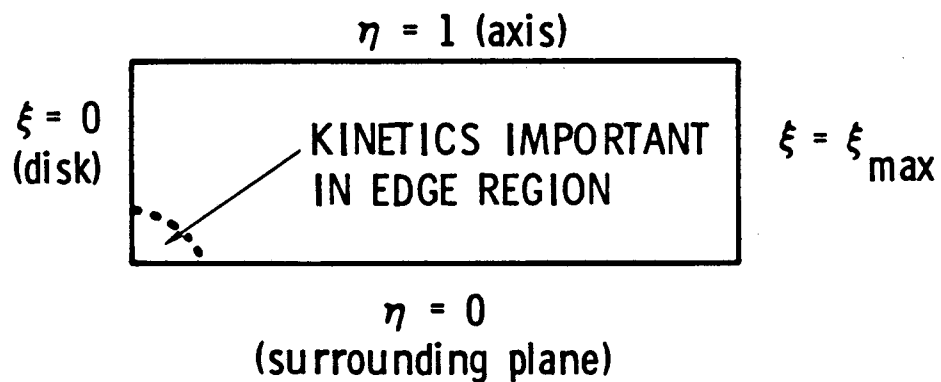


FIGURE 2. THE DISK-PLANE SYSTEM TRANSFORMS TO A RECTANGULAR REGION IN ROTATIONAL ELLIPTIC COORDINATES WITH THE DISK COMPLETELY OCCUPYING ONE END OF THE RECTANGLE

c. the potential approaches the primary distribution both as ξ becomes large and as η approaches 1 (the disk axis). This boundary condition will be expressed more quantitatively below.

Conventionally, the potential Φ is taken to be zero far from the disk ($\xi \rightarrow \infty$). Because the emphasis here is on the edge region, it is convenient to define a dimensionless potential ϕ as

$$\phi = \frac{\pi}{4} \left(1 - \Phi/\Phi_0^p \right) = \frac{\pi}{4} - \frac{\kappa\Phi}{r_0^2 i_{avg}} , \quad (9)$$

where

$$\Phi_0^p = I/4\kappa r_0 \quad (10)$$

is the value of Φ at the disk surface for the primary distribution and I is the total current to the disk ($= \pi r_0^2 i_{avg}$).

In order to emphasize the corner region, the stretched variables given below were adopted:

$$\bar{\xi} = \delta\xi \quad (11)$$

$$\bar{\eta} = \delta\eta . \quad (12)$$

In the region of interest, $\bar{\eta}$ and $\bar{\xi}$ will be of order unity, and the behavior of ϕ will be such that the stretched potential variable

$$\bar{\phi} = \delta\phi - \ln(\delta) \quad (13)$$

will be appropriate for the edge region as well.

With the change of variables, Laplace's equation becomes

$$(\delta^2 - \bar{\eta}^{-2}) \frac{\partial^2 \bar{\phi}}{\partial \bar{\eta}^2} - 2\bar{\eta} \frac{\partial \bar{\phi}}{\partial \bar{\eta}} + (\delta^2 + \bar{\xi}^2) \frac{\partial^2 \bar{\phi}}{\partial \bar{\xi}^2} + 2\bar{\xi} \frac{\partial \bar{\phi}}{\partial \bar{\xi}} = 0 . \quad (14)$$

Since $\bar{\eta}$ and $\bar{\xi}$ and the derivatives are of order unity in the edge region and δ is taken to be large, only the terms multiplied by δ^2 need be retained. With this approximation, Laplace's equation reduces to

$$\frac{\partial^2 \bar{\phi}}{\partial \bar{\eta}^2} + \frac{\partial^2 \bar{\phi}}{\partial \bar{\xi}^2} = 0 . \quad (15)$$

The boundary conditions become:

a. at $\bar{\xi} = 0$

$$\frac{i_n}{\delta i_{avg}} = \frac{1}{2} E e^{\bar{\phi}_0} = \frac{1}{\eta} \left. \frac{\partial \bar{\phi}}{\partial \bar{\xi}} \right|_{\bar{\xi}=0} , \quad (16)$$

where E is a parameter of the system defined by the equation

$$E = 2 \frac{i_0}{i_{avg}} \exp \left[\frac{\alpha_a F}{RT} (V - \Phi_0^p) \right] . \quad (17)$$

Since E involves both i_{avg} and V , which cannot be specified independently, it will need to be determined. Its value will be discussed below and in Appendix A.

b. at $\bar{\eta} = 0$

$$\frac{\partial \bar{\phi}}{\partial \bar{\eta}} = 0 . \quad (18)$$

c.

$$\frac{\partial \bar{\phi}}{\partial \bar{\xi}} \rightarrow \frac{1}{2} \text{ as } \bar{\eta}^{-2} + \bar{\xi}^2 \rightarrow \infty . \quad (19)$$

The last condition comes from matching with the primary distribution,

a refinement of the original boundary condition c. The primary distribution for the potential is¹

$$\phi^p = \frac{1}{2} \tan^{-1} \xi , \quad (20)$$

and at the electrode

$$\frac{i_n}{i_{avg}} = \frac{1}{2\eta} . \quad (21)$$

The behavior of equation 20 at small ξ leads to the matching condition in equation 19.

The problem of the current and potential distributions has been split into two problems, or a problem in two regions. In the first region, far from the corner region, the current and potential are given by the primary distributions, which may be obtained by neglecting the effect of electrode kinetic boundary conditions. In the region near the corner ($\bar{\eta} = \bar{\xi} = 0$), kinetics are important, but certain terms of Laplace's equation may be neglected. This has the classic form of a singular-perturbation problem, which is solved subject to the requirement that the solutions for the two regions must "match" at the overlap of the regions.

For this to be a well-posed, singular-perturbation problem, the differential equation and boundary conditions must be independent of the perturbation parameter, $1/\delta$. This requirement is met except for equation 16, which involves the parameter E . From equation 17, it can be seen that E' is a function of δ , in general. However, as shown in Appendix A, $\ln E$ approaches unity for large values of δ (see equation A19). This approximation was adopted for the calculations, and it

will be discussed again later. The present problem for large δ is different from that for large J primarily because of the boundary condition 16. The variable transformations are different as well, but the transformed equation 15 and the other boundary conditions are similar.

The solution to the problem was obtained by the method of finite differences with successive overrelaxation. Reference 4 gives details of expressing the differential equation in finite-difference form, as well as some description of the method of successive overrelaxation. The highly nonlinear boundary condition, equation 16, was treated for successive iterations by the method described in reference 4.

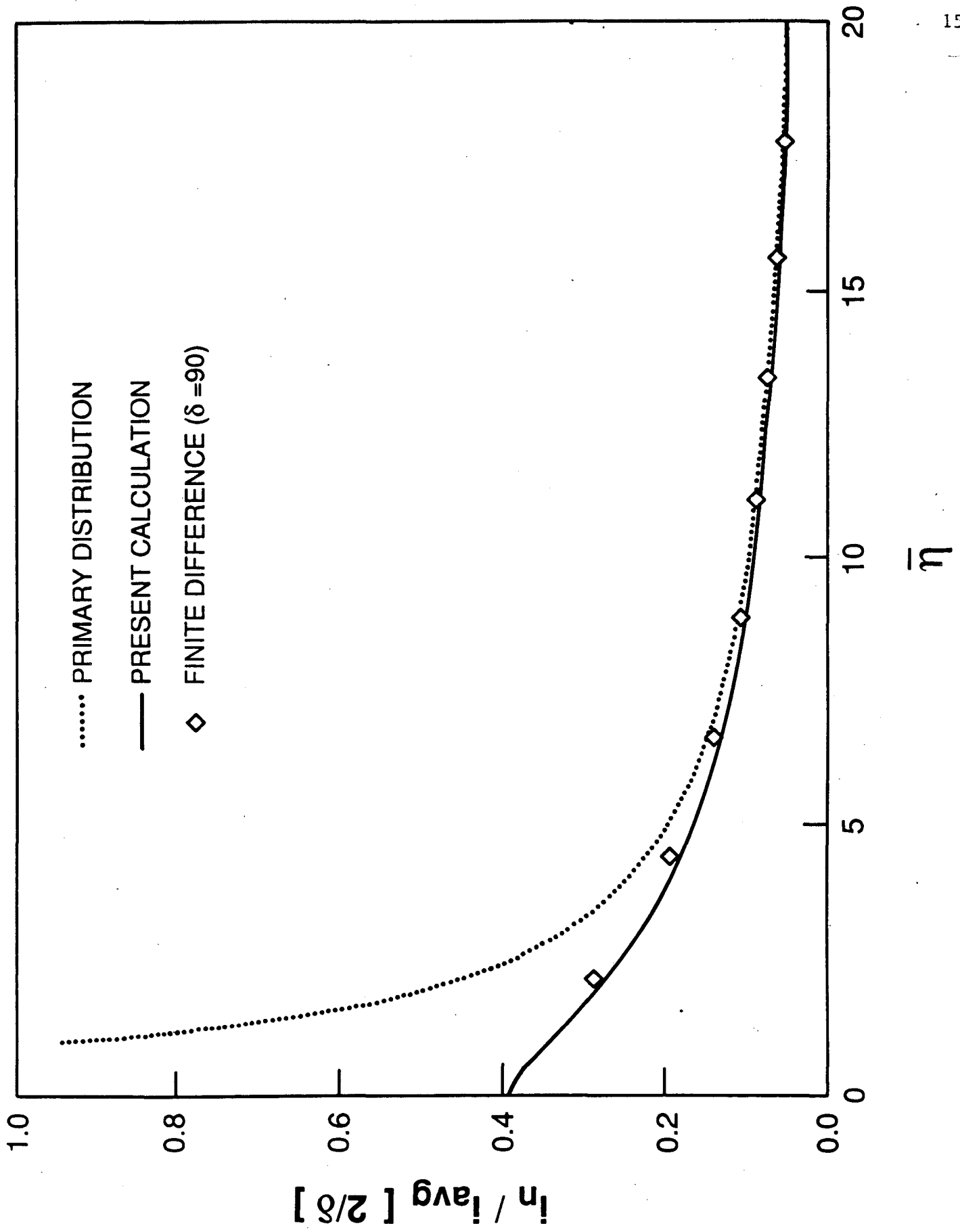
It was found that boundary condition c did not adequately specify the behavior of $\bar{\phi}$ at large values of $\bar{\eta}$ and $\bar{\xi}$ for numerical calculations. The asymptotic form of $\bar{\phi}$ was consequently obtained from the specific problem statement at large $\bar{\eta}$ and $\bar{\xi}$, as developed in Appendix B. The result in equation B8 has a constant, A_1 , whose value had to be determined. Equation B8 was differentiated with respect to $\bar{\eta}$, and A_1 was eliminated between this equation and equation B8 to give a relationship between the potential and its derivative at large values of $\bar{\eta}$. The resulting equation for the derivative of $\bar{\phi}$ was used (in finite-difference form) on the boundary at large values of $\bar{\eta}$. A similar technique was used to develop an equation for the partial derivative with respect to $\bar{\xi}$ for the boundary at large $\bar{\xi}$. The procedure proved to be satisfactory, and the calculation of $\bar{\phi}$ was readily performed.

It was further found to be expedient to use the linear coordinates out to $\bar{\xi} = \bar{\eta} = 1$, but logarithmic coordinates for larger values (i.e., $\ln\bar{\xi}$, $\ln\bar{\eta}$ for $\bar{\xi}$, $\bar{\eta} \geq 1$). The two coordinate systems coincide at $\bar{\eta} = 1$ and at $\bar{\xi} = 1$. This procedure provided a large number of points in the region for small $\bar{\eta}$ and $\bar{\xi}$ where $\bar{\phi}$ changed the most, and a fewer number of mesh points in the region where the change was much smaller. This scheme worked very well, even with successive overrelaxation in the iteration process. Such mixed coordinates were also used by Newman *et al.*⁸ for a pit geometry.

Results and Discussion

The results presented below are general, i.e., dimensionless, and are independent of system parameters. This means that the results may be used for any and all large values of δ . They may be used in conjunction with the results of Nişancıoğlu and Newman⁵ for a complete description of the current and potential distributions on electrodes at high current densities, in the absence of diffusion effects. The accuracy of the results was checked by changing the mesh size and convergence parameter and changing the position of the outer boundaries. The calculated values of $\bar{\phi}$ are estimated to be accurate to within 0.1 to 0.3 percent.

The distribution of i_n/i_{avg} along the electrode surface is shown in figure 3 and compared to the primary distribution. Also plotted are results of ordinary finite-difference calculations, but for large δ ($\delta = 90$), according to reference 4. (These data are plotted in fig-



ure 1 as well.) As expected, the current density is finite at the edge of the electrode in contrast to the primary distribution, and the two distributions converge far from the edge. The two differ by only 0.1 percent at $\bar{\eta} = 50$ ($\bar{\xi} = 0$). The value of $\bar{\phi}_0$ at the edge (i.e., $\bar{\xi} = 0$, $\bar{\eta} = 0$) was found to be -1.9350, and thus

$$\frac{2}{\delta E} \frac{i_{edge}}{i_{avg}} = e^{\bar{\phi}_0} \Big|_{edge} = 0.1444 . \quad (22)$$

Equation 22 provides a general relationship which may be used to calculate the current density at the disk edge for any (large) value of δ .

Tafel kinetics have been used for the present investigation and yield a relationship of the form

$$\frac{i_{edge}}{i_{avg}} = 0.1963 \delta . \quad (23)$$

This may be compared with equation 3 for linear kinetics, but it should be noted that the dependence on the polarization parameters is different for the two cases. It has been popular in the literature to linearize Tafel kinetics for cases where the potential across the electrode surface does not vary too much about some average value. Such an approximate relationship for linearized Tafel kinetics would yield

$$\frac{i_{edge}}{i_{avg}} \propto \sqrt{\delta} . \quad (24)$$

By comparison to equation 23, linearization is not a good approximation for this case. This is because the current density varies by

quite significant amounts from the average value. At the center of the disk

$$\frac{i_n}{i_{avg}} \rightarrow \frac{1}{2},$$

but at the edge, the ratio is given by equation 23. Therefore, the variation in current density between center and edge increases linearly with increasing δ .

The distribution of potential across the surface is also of interest. The potential we are discussing here is the potential in solution just outside the electrical double layer (a distance of about 10 to 100 Å from the surface). The potential in the metal has been designated as V , and is uniform everywhere on the metal surface. From the results above it may be shown that for large δ ,

$$\Delta\phi_0 = \frac{\kappa\Delta\Phi_0}{r_0 i_{avg}} = \frac{\ln(0.39\delta)}{\delta}, \quad (25)$$

where Δ denotes the difference between values at the center and the edge of the disk. This quantity has the value⁹ 0.363 at low values of δ , where a uniform current distribution prevails, but for large values of δ it approaches zero, appropriate for the primary distribution. Equation 25 describes specifically how the potential distribution approaches the primary distribution, which may be used as a good approximation over much of the electrode. An estimate of how much of the electrode is affected is provided by Figure 3 and the variable η . The affected region is dependent on δ , through $\bar{\eta}$, and the figure provides the general solution for any large value of δ . The edge region

is thus defined by $r_0 - r = O(r_0/\delta^2)$.

Figure 4 expresses some of these potential relations from a different point of view. The stretching of potential inherent in $\bar{\phi}$ (see equation 13) means that variations of $\bar{\phi}$ describe variations of $\alpha_a F\bar{\phi}/RT$, a nondimensionalization that seems appropriate for the kinetic expression in equation 1. Figure 4 shows potentials for the electrode and for the solution at both the center and the edge of the disk, as calculated by the method of reference 2. These are compared with asymptotes for large δ as deduced in the present work.

The slope of $\alpha_a F(V - \Phi_0^P)/RT$ versus $\ln(\delta)$ is unity at both small and large δ , but the intercept shifts because E changes from 1 at low δ to e at high δ (see appendix A). The potential $\Phi_0 - \Phi_0^P$ at the center shifts from zero at low δ to $RT/\alpha_a F$ at large δ . To infer this latter value requires one to ascertain the value of E as well as the fact that i_n/i_{avg} approaches 0.5 at the center. At the edge, $\alpha_a F(\Phi_0 - \Phi_0^P)/RT$ is zero at low δ and approaches the asymptote $1.935 - \ln(\delta)$ at high δ . The calculations according to the method in reference 2 are unable to give correct results for δ values above about 90, but the approach to the asymptotes is apparent.

While $\kappa\Delta\Phi_0/r_0 i_{avg}$ approaches zero for large δ , $\alpha_a F\Delta\Phi_0/RT$ increases. Figure 4, by the vertical distances between the curve for V and those for Φ_0 , can give an impression of how the overpotential η_s changes with δ at the center and the edge of the disk. At the center, i_n increases as $0.5i_{avg}$, and the increase in overpotential is achieved by an increase in $V - \Phi_0^P$. At the edge, i_{edge} increases in proportion to

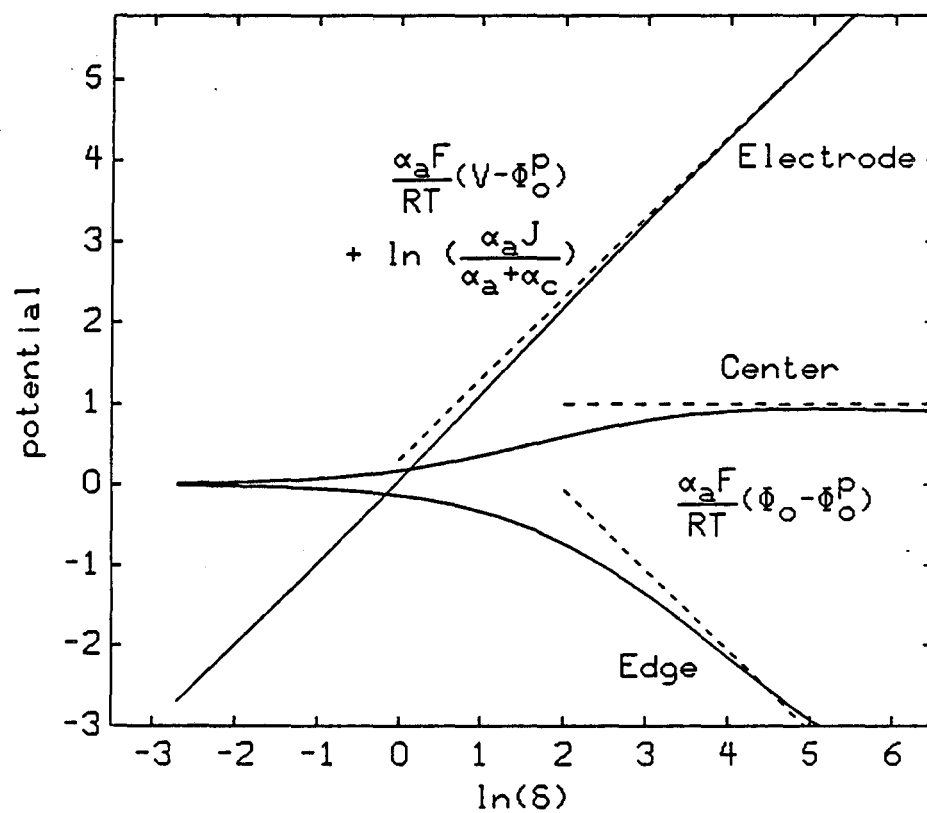


Figure 4. Comparison of potentials of electrode and solution at edge and center of disk as functions of δ with asymptotes valid at high values of δ .

the square of i_{avg} , and this requires both an increase in $V-\Phi_0^P$ and a decrease in $\Phi_0-\Phi_0^P$.

It should be anticipated that the present results can be used to describe the edge effects for high current densities and Tafel kinetics for other geometries as well. In particular, equation 23 can be used to express the dependence of the current distribution on the parameter δ , although a slightly different constant may be used for other geometries. Each geometry will have a different characteristic length for calculations of δ as well.

Wagner⁶ obtained an expression which approximated the edge current density at planar electrodes for linear kinetics of the form

$$\frac{i_{edge} - i_{avg}}{i_{avg}} = \frac{3^{3/4}}{\pi\sqrt{2}} \sqrt{J} = 0.513 \sqrt{J}, \quad (26)$$

where the original symbols have been converted to those used in the present paper.* This equation should be compared to equation 3. The two have the same square-root dependence on the parameter J and differ only in the constant. This provides some justification for extrapolating the singular-perturbation results to electrode geometries other than the disk. Each geometry would have its own characteristic length used to calculate J . An expression analogous to equation 3 would be generated for each geometry and would also be expected to depend on \sqrt{J} , but with a different value of the multiplying constant. Finally, it should be noted that the relationship (equation 26) derived by

* J in equation 26 has the characteristic length L of the planar electrode instead of r_0 , which is the characteristic length for a disk electrode.

Wagner⁶ seems to be approximate, and its derivation is not clear in the original paper.

Extension to Other Geometries

The results from this work at high current densities and those of Nişancıoğlu and Newman⁵ for high exchange current densities ought to be made quantitatively applicable to other geometries. The salient feature is that these results deal with the edge region, where the potential distribution away from the edge closely follows a primary (or ohmically-limited) distribution. In the edge region, the edge itself appears to be straight, and the electrode and the insulator lie in a plane (*i.e.*, form an angle of 180°).

If we had solutions in an edge region for high δ or J for other geometries, we could probably extend the results. Such geometries could include a region where the electrode and the insulator form an angle different from 180° or for the corner of a square electrode lying in a plane with an insulator. However, for the moment we must restrict ourselves to the geometry as stated.

The salient feature of the geometry can be restated in terms of the normal component of the primary current distribution i_n^P on an electrode:

$$i_n^P = P/\sqrt{x} , \quad (27)$$

where x is the distance along the electrode from its edge and P is a constant characterizing the primary distribution for the particular

geometry and applied potential. In particular, we seek to phrase the situation near the edge so as to be independent of the overall electrode size, its placement relative to the other electrode(s), and the applied potential. The variation of the potential near the electrode should be expressible in terms of P , the conductivity κ , and the distance z perpendicular to the electrode as well as x and the kinetic parameters (for either Tafel or linear kinetics). As a specific challenge, we can try to apply the disk results discussed above to two-dimensional situations of a planar electrode of length L embedded in a plane or to two electrodes of length L embedded in the walls of a flow channel and placed opposite to each other at a distance of h . Wagner⁶ gave us the primary current distribution for the former case; Newman⁹ for the latter.

To establish the connection, we can first expand equation 2 in the edge region and show that

$$P = i_{avg} \sqrt{r_0/8} \quad (28)$$

for the disk geometry. Along the electrode, then, $\bar{\eta}$ is related to x by

$$\bar{\eta} = \frac{4\alpha_a F}{RT\kappa} P \sqrt{x} \quad (29)$$

and this can be interpreted as a more general abscissa scale for figure 3. The ordinate scale should be interpreted according to

$$\frac{2i_n}{\delta i_{avg}} = \frac{RT\kappa}{4\alpha_a F} \frac{i_n}{P^2} \quad (30)$$

and consequently the maximum current, at the electrode edge, is

$$i_{edge} = 1.57 \frac{\alpha_a FP^2}{RT\kappa} \quad (31)$$

For the channel geometry, there is an additional geometric parameter:

$$\epsilon = \pi L/2h, \quad (32)$$

and the primary distribution⁹ near the edge allows us to deduce that

$$P = i_{avg} \frac{\sqrt{\epsilon L / \tanh \epsilon}}{2K(\tanh^2 \epsilon)}, \quad (33)$$

where $K(m)$ is the complete elliptic integral of the first kind, tabulated in reference 10. For the limiting case of $\epsilon \rightarrow 0$, the counterelectrode is far away, and

$$P \rightarrow i_{avg} \frac{\sqrt{L}}{\pi} \quad (34)$$

For a thin-gap cell, $\epsilon \rightarrow \infty$, and

$$P \rightarrow i_{avg} \sqrt{h/2\pi} \quad (35)$$

These last two equations can be verified independently from equations 33 and 66 of Wagner.⁶ For Tafel kinetics at high average current densities, equations 33 and 31 can be combined with the relationship between i_{avg} and i_{min} for this system to yield

$$\frac{i_{edge}}{i_{min}} = \frac{0.39\delta}{K(\tanh^2 \epsilon)} \quad (36)$$

Figure 6 of Parrish and Newman¹¹ confirms that i_{edge}/i_{min} is substantially a linear function of δ even down to $\delta = 0$. If we add unity to the right side of equation 36 and take account of the absence of the factor α_a in Parrish and Newman's definition of δ , we can

calculate straight lines which nearly coincide with those on their figure 6 for $h/L = 0.5, 1, \text{ and } \infty$.

For linear kinetics at high exchange current densities and the disk geometry, Nişancıoğlu and Newman⁵ gave us equation 3. From equation 28, we obtain the generalization

$$i_{edge} = 1.75 P \sqrt{\alpha_a + \alpha_c} \left(\frac{Fi_0}{RT\kappa} \right)^{1/2} \quad (37)$$

The abscissa on figure 3 of Nişancıoğlu and Newman should be interpreted, in general, as

$$\bar{\eta} = \sqrt{\alpha_a + \alpha_c} \left(\frac{2Fi_0 x}{RT\kappa} \right)^{1/2} \quad (38)$$

while the ordinate should be interpreted as

$$\bar{\phi}_0 = \left(\frac{1}{\alpha_a + \alpha_c} \frac{RT\kappa}{2Fi_0} \right)^{1/2} \frac{i_n}{P} \quad (39)$$

For the channel geometry, at high exchange current densities, equations 33 and 37 can be combined with the relationship between i_{avg} and i_{min} for this system to yield

$$\frac{i_n}{i_{min}} = \left(\frac{J \tanh \epsilon}{2\epsilon} \right)^{1/2} \bar{\phi}_0 \quad (40)$$

Here J is formed with the electrode length L instead of r_0 . With a maximum value of 1.24 for $\bar{\phi}_0$, and for the case where $h \gg L$,

$$i_{edge}/i_{avg} = 0.558 \sqrt{J} \quad (41)$$

The coefficient obtained by Wagner in equation 26 is 8 percent lower, which is surprisingly good agreement in view of the approximation in

his analysis. He also treated thin-gap cells and presented i_{edge}/i_{avg} graphically versus J . Equation 40 can also be used to extend the results in figure 4 of Parrish and Newman to higher values of J .

Summary

A singular-perturbation analysis has been used to develop a treatment for the current density at the edge of a disk electrode for high average current density, high compared to $RT\kappa/\alpha_a Fr_0$ and high compared to the exchange current density. A finite-difference, numerical technique was used to obtain a solution. This solution is quite general and is valid for any and all large values of δ . The results provide a definitive description of the way in which the current and potential distributions approach the primary distributions as δ increases.

Acknowledgment

This work was supported by the U. S. Department of Energy under Contract No. DE-AC04-76-DP00789 and the Assistant Secretary for Conservation and Renewable Energy, Office of Energy Storage and Distribution of the U. S. Department of Energy under Contract No. DE-AC03-76SF00098.

List of Symbols

A_i	constants for the series in equation B2
E	dimensionless parameter (see equation 17)
F	Faraday's constant, 96487 C/equiv
h	distance separating walls of channel cell, cm
i_0	exchange current density, A/cm^2
i_{avg}	current density averaged over the electrode surface, A/cm^2
i_{edge}	value of i_n at the edge of an electrode, A/cm^2
i_n	current density normal to the electrode surface, A/cm^2
I	total current to the disk electrode, A
J	dimensionless polarization parameter for linear electrode kinetics
L	electrode length for channel cell, cm
P	parameter characterizing the primary current distribution near the edge of an electrode, $A/cm^{1.5}$
r	radial position measured from the center of the disk, cm
r_0	electrode radius, cm
R	universal gas constant, 8.3143 J/mol·K

T	absolute temperature, K
x	distance along electrode from its edge, cm
V	potential of the disk electrode, V
z	distance normal to the electrode surface, cm

Greek letters

α_a, α_c	transfer coefficients for anodic or cathodic processes
δ	dimensionless polarization parameter for Tafel electrode kinetics
ϵ	length ratio for channel geometry
η_s	surface overpotential, V
κ	specific conductivity, $\text{ohm}^{-1} \cdot \text{cm}^{-1}$
ξ, η	rotational elliptic coordinates
ϕ	dimensionless potential
$\bar{\phi}, \bar{\eta}, \bar{\xi}$	stretched potential and coordinates
Φ	electric potential, V
Φ_0	value of Φ at electrode surface, V

Superscripts

p	refers to primary distribution
-----	--------------------------------

References

1. John Newman, "Resistance for Flow of Current to a Disk," *J. Electrochem. Soc.*, 113 (1966), 501-502.
2. John Newman, "Current Distribution on a Rotating Disk below the Limiting Current," *J. Electrochem. Soc.*, 113 (1966), 1235-1241.

3. Leonard Nanis and Wallace Kesselman, "Engineering Applications of Current and Potential Distributions in Disk Electrode Systems," *J. Electrochem. Soc.*, 118 (1971), 454-461.
4. William H. Smyrl and John Newman, "Current and Potential Distributions in Plating Corrosion Systems," *J. Electrochem. Soc.*, 123 (1976), 1423-1432.
5. Kemal Nişancıoğlu and John Newman, "The Short-Time Response of a Disk Electrode," *J. Electrochem. Soc.*, 121 (1974), 523-527.
6. Carl Wagner, "Theoretical Analysis of the Current Density Distribution in Electrolytic Cells," *J. Electrochem. Soc.*, 98 (1951), 116-128.
7. John Newman, "The Fundamental Principles of Current Distribution and Mass Transport in Electrochemical Cells," Allen J. Bard, ed., *Electroanalytical Chemistry* (New York: Marcel Dekker, Inc., 1973), 6, 187-352.
8. John Newman, D. N. Hanson, and K. Vetter, "Potential Distribution in a Corroding Pit," *Electrochim. Acta*, 22 (1977), 829-831.
9. John S. Newman, *Electrochemical Systems* (Englewood Cliffs, N. J.: Prentice-Hall, Inc., 1973), pp. 342, 350.
10. Milton Abramowitz and Irene A. Stegun, eds., *Handbook of Mathematical Functions* (Washington: National Bureau of Standards, 1964), p. 608.
11. W. R. Parrish and John Newman, "Current Distributions on Plane, Parallel Electrodes in Channel Flow," *J. Electrochem. Soc.*, 117

(1970), 43-48.

Appendix A. Dependence of the Parameter E on δ

We begin with the identity, peculiar to a disk geometry,

$$\int_0^1 \phi_0 d\eta = 0 \quad (\text{A1})$$

and define

$$\int_0^\eta \phi_0 d\eta = I(\eta) = \frac{1}{\delta^2} \int_0^\eta [\bar{\phi}_0 + \ln \delta] d\bar{\eta} . \quad (\text{A2})$$

The latter part of equation A2 is appropriate for the inner region near the corner.

In the outer region, we denote the quantity I as \bar{I} , and write

$$\bar{I}(\eta) = I(1) - \int_\eta^1 \phi_0 d\eta . \quad (\text{A3})$$

Here the potential function should be expanded in the perturbation series

$$\bar{\phi} = \phi = \phi^P + \frac{1}{\delta} \bar{\phi}^0 + F(\delta) \bar{\phi}^1 + \dots \quad (\text{A4})$$

ϕ^P is given by equation 20, and we note that

$$\phi_0^P = 0 \quad \text{and} \quad \left. \frac{\partial \phi^P}{\partial \xi} \right|_{\xi=0} = \frac{1}{2} . \quad (\text{A5})$$

The functions $\bar{\phi}^0$ and $\bar{\phi}^1$ and $F(\delta)$ are unknown at this point and are to be determined from the original differential equation and either the boundary conditions or the matching condition. For the purposes of this paper, it will only be necessary to determine $\bar{\phi}^0$ and the order of

magnitude of $F(\delta)$. We tentatively expect $F(\delta)$ to be of order $(1/\delta^2)$.

Boundary condition 16 provides the equation for the potential written for the outer region

$$\frac{1}{2} E e^{\delta\phi_0} = \frac{1}{\eta} \frac{\partial\phi}{\partial\xi} \Big|_{\xi=0} \quad (\text{A6})$$

Substitution of equations A4 and A5 gives

$$\frac{1}{2} E e^{(\bar{\phi}_0^0 + \delta F(\delta)\bar{\phi}_0^1)} = \frac{1}{2\eta} + \frac{1}{\delta\eta} \frac{\partial\bar{\phi}^0}{\partial\xi} + \frac{F(\delta)}{\eta} \frac{\partial\bar{\phi}^1}{\partial\xi} \quad (\text{A7})$$

The derivatives on the right side are to be evaluated at $\xi = 0$. This equation can be rearranged to yield

$$e^{(\ln\eta E + \bar{\phi}_0^0 + \delta F(\delta)\bar{\phi}_0^1)} = 1 + \frac{2}{\delta} \frac{\partial\bar{\phi}^0}{\partial\xi} + 2F(\delta) \frac{\partial\bar{\phi}^1}{\partial\xi} \quad (\text{A8})$$

If we are to match orders in δ , we must have

$$\bar{\phi}_0^0 = -\ln(\eta E) \quad (\text{A9})$$

so that equation A9 becomes

$$e^{\delta F(\delta)\bar{\phi}_0^1} = 1 + \frac{2}{\delta} \frac{\partial\bar{\phi}^0}{\partial\xi} + 2F(\delta) \frac{\partial\bar{\phi}^1}{\partial\xi} \quad (\text{A10})$$

Expanding the exponential, we see that

$$F(\delta) = O(1/\delta^2) \quad (\text{A11})$$

by equating like powers of δ .

Introducing the relationships for $\bar{\phi}_0^0$ and $F(\delta)$ into equation A3, we get

$$\bar{I}(\eta) = - \int_{\eta} \left[\frac{-1}{\delta} \ln(\eta E) + \frac{1}{\delta^2} \bar{\phi}_0^1 \right] d\eta$$

$$= \frac{1}{\delta} \left[\ln E - 1 + \eta - \eta \ln(\eta E) \right] - \frac{1}{\delta^2} \int_{\eta}^1 \bar{\phi}_0^1 d\eta . \quad (\text{A12})$$

In terms of $\bar{\eta}$ and in the limit as $\eta \rightarrow 0$, this becomes

$$\lim_{\eta \rightarrow 0} \bar{I}(\eta) = \frac{1}{\delta} \left[\ln E - 1 \right] + \frac{\bar{\eta}}{\delta^2} [1 - \ln(\bar{\eta} E / \delta)] - \frac{1}{\delta^2} \int_0^1 \bar{\phi}_0^1 d\eta . \quad (\text{A13})$$

In the inner region we denote I as $\bar{I}(\bar{\eta})$. The potential in the inner region should be expanded as

$$\bar{\phi} = \bar{\phi}^0 + G(\delta) \bar{\phi}^1 + \dots \quad (\text{A14})$$

$G(\delta)$ is expected to be $O(1/\delta)$, and the function $\bar{\phi}^1$ is unknown. The asymptotic form for $\bar{\phi}_0^0$ is given in Appendix B as

$$\bar{\phi}_0^0 = -\ln(E\bar{\eta}) + \frac{2A_1}{\bar{\eta}^2} \quad \text{for } \bar{\eta} \gg 1 . \quad (\text{A15})$$

Introduction of these functions into equation A2 gives

$$\begin{aligned} \bar{I}(\bar{\eta}) &= \frac{\bar{\eta}}{\delta^2} [1 - \ln(E\bar{\eta}/\delta)] \\ &+ \frac{1}{\delta^2} \int_0^{\bar{\eta}} [\bar{\phi}_0^0 + \ln(E\bar{\eta})] d\bar{\eta} + \frac{G(\delta)}{\delta^2} \int_0^{\bar{\eta}} \bar{\phi}_0^1 d\bar{\eta} + \dots \end{aligned} \quad (\text{A16})$$

The matching condition is expressed by

$$\lim_{\bar{\eta} \rightarrow \infty} \bar{I}(\bar{\eta}) = \lim_{\eta \rightarrow 0} \bar{I}(\eta) . \quad (\text{A17})$$

The two expressions in equations A13 and A16 are supposed to match to all orders in both δ and $\bar{\eta}$. We can see that the first term in equation A16 is identical to the second term in equation A13. Furthermore, the position or η dependence must match automatically, and the

matching really determines the constant E to a certain order in δ . The asymptotic form in equation A15 guarantees that the upper limit on the first integral in equation A16 can be extended to infinity. We thus obtain for E :

$$\ln E = 1 + \frac{1}{\delta} \left\{ \int_0^{\infty} [\bar{\phi}_0^0 + \ln(E\bar{\eta})] d\bar{\eta} + \int_0^1 \bar{\phi}_0^1 d\eta \right\} + O(G(\delta)/\delta) . \quad (\text{A18})$$

Rather than evaluate the terms in brackets, we write

$$\ln E = 1 + O(1/\delta) + \dots \quad (\text{A19})$$

Figure 5 shows how $2/E$ depends on δ . This ratio can be regarded as the ratio of the current to that which would be expected if the applied potential in excess of the primary potential Φ_0^p could be used in the kinetic expression. The calculation method, similar to that used in reference 2 for problems of the secondary current distribution, confirms that $2/E$ approaches $2/e = 0.73576$ as δ becomes large, although there is a small distortion at large δ .

Appendix B. Behavior of $\bar{\phi}$ at Large Values of $\bar{\eta}$ and $\bar{\xi}$

The boundary condition 19 was found to be inadequate to produce reliable results from the finite-difference calculations. In particular, applying this condition at the maximum values of $\bar{\eta}$ and $\bar{\xi}$, for different positions of these boundaries, caused changes in the calculated values of $\bar{\phi}$ throughout the domain. Of special concern were the changes in the values of i_n/i_{avg} and $\bar{\phi}_0$ on the electrode surface.

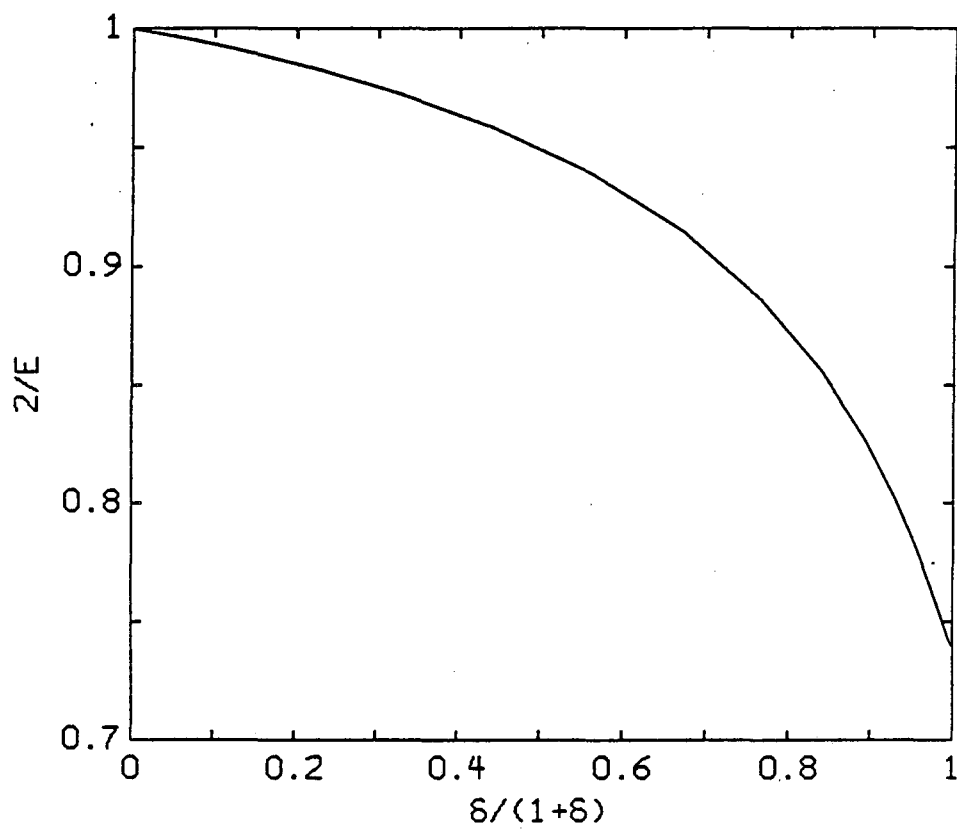


Figure 5. Approach of E to e at large δ .

The behavior of $\bar{\phi}$ at large $\bar{\eta}, \bar{\xi}$ was treated by using the coordinates

$$r^* = (\bar{\eta}^2 + \bar{\xi}^2)^{1/2}$$

$$\theta^* = \tan^{-1}(\bar{\eta}/\bar{\xi}) .$$

Laplace's equation for $\bar{\phi}$ in the inner region as given in equation 17 is then

$$\frac{1}{r^*} \frac{\partial}{\partial r^*} \left[r^* \frac{\partial \bar{\phi}}{\partial r^*} \right] + \frac{1}{r^{*2}} \frac{\partial^2 \bar{\phi}}{\partial \theta^{*2}} = 0 , \quad (\text{B1})$$

with the general solution, satisfying conditions 18 and 19,

$$\bar{\phi} = A_0 - \ln(Er^*) + \frac{1}{2} r^* \cos \theta^* + \sum_{k=1}^{\infty} A_k (r^*)^{-k} \cos(k\theta^*) . \quad (\text{B2})$$

The coefficient of $\ln r^*$ has also been set according to the requirements of boundary condition 16. This last condition, on the electrode at $\bar{\xi} = 0$, becomes

$$\frac{1}{2} r^{*2} E e^{\bar{\phi}_0} = - \left. \frac{\partial \bar{\phi}}{\partial \theta^*} \right|_{\theta^* = -\pi/2} = \frac{1}{2} r^* + \sum_{\substack{k=1, \\ 3,5}} \frac{k A_k}{r^{*k}} (-1)^{(k-1)/2} \quad (\text{B3})$$

or

$$\frac{1}{2} e^{A_0} \exp \left[- \frac{A_2}{r^{*2}} + \frac{A_4}{r^{*4}} + \dots \right] = \frac{1}{2} + \frac{A_1}{r^{*2}} - \frac{3A_3}{r^{*4}} + \dots \quad (\text{B4})$$

The exponential may be expanded for large r^* to yield

$$A_0 = 0 , \quad (\text{B5})$$

$$A_2 = -2A_1 , \quad (\text{B6})$$

$$A_4 = -6A_3 - \frac{1}{2} A_2^2 . \quad (\text{B7})$$

This allows the expression for $\bar{\phi}$ to be written in terms of the original variables $\bar{\eta}, \bar{\xi}$ as

$$\bar{\phi} = \frac{1}{2} \bar{\xi} - \ln E(\bar{\eta}^{-2} + \bar{\xi}^{-2})^{1/2} + \frac{A_1 \bar{\xi}}{\bar{\xi}^{-2} + \bar{\eta}^{-2}} - \frac{2A_1(\bar{\xi}^{-2} - \bar{\eta}^{-2})}{(\bar{\xi}^{-2} + \bar{\eta}^{-2})^2} + \dots \quad (\text{B8})$$

Equation B8 is valid for large $\bar{\eta}, \bar{\xi}$. The expression provided a satisfactory boundary condition for the numerical calculations. The constant A_1 was determined from the calculated $\bar{\phi}$ array and found to be constant for large $\bar{\eta}, \bar{\xi}$, with the value $A_1 = -3.1$. If equation B8 was used as a boundary condition for large $\bar{\eta}$ and $\bar{\xi}$, rather than the form described in the text where A_1 was eliminated, a variation of 10 percent in A_1 caused a negligible change in the calculated values of $\bar{\phi}$, i.e., the calculations were not very sensitive to A_1 .

*LAWRENCE BERKELEY LABORATORY
TECHNICAL INFORMATION DEPARTMENT
UNIVERSITY OF CALIFORNIA
BERKELEY, CALIFORNIA 94720*